

The Effect of Water Speed on Bottom Contact and Escapement
Under the Footrope of a Survey Trawl

Kenneth L. Weinberg and David A. Somerton

Abstract

Towing speed on bottom trawl surveys is usually designated in terms of speed over ground (SOG) rather than speed through the water (STW). However, STW is likely more influential on catchability because of its more pronounced effects on trawl geometry and fish swimming speed. We conducted a 2-phase experiment to investigate: 1) the effect of STW on the footrope bottom contact of our standard survey trawl; and 2) the effect of STW on the capture efficiency of the same trawl. Speed through water was measured with a trawl-mounted current meter; distance of the footrope off-bottom was measured with a bottom contact sensor. Capture efficiency was estimated by catching the fish escaping beneath the footrope with an auxiliary net. During Phase I, bottom contact in the center of the footrope of our survey trawl was unstable at the survey towing speed of 3 knots and declined with increasing STW. At STW of 4.5 knots and above the trawl likely lifted completely off-bottom. During Phase II, capture efficiency declined with STW for two flatfish species and a combined skate group *Bathyraja* spp, but this decline varied with body size. Capture efficiency did not change as a function of STW for two species of gadids, Pacific cod *Gadus macrocephalus* and walleye pollock *Theragra chalcogramma* and a large flatfish species, Pacific halibut *Hippoglossus stenolepis*. Our results indicate that in areas subject to strong current, variation in survey CPUE could be reduced for some species by standardizing towing speed to speed through water rather than speed over ground.

Kenneth L. Weinberg, David Somerton: National Marine Fisheries Service, Alaska Fisheries Science Center, 7600 Sand Point Way NE, Seattle, WA 98115-0070, USA [tel: +1 206 526 6109; fax +1 206 526 6723, email: ken.weinberg@noaa.gov ; david.somerton@noaa.gov]

Introduction

Fishing gear and procedures are standardized on bottom trawl surveys to help reduce the variation in catch per unit effort (CPUE) that is due to variation in trawl efficiency. Among the standardized fishing procedures, towing speed is perhaps one of the more influential due to its effects on trawl geometry and fish swimming speed. Speed over ground (SOG), measured with global positioning system (GPS), is the most common method used for determining towing speed (Shaw et al. 2000, ICES 1999), even though speed through the water (STW) largely determines trawl geometry (Fridman 1986). Maintaining constant STW, rather than constant SOG, might reduce variability in trawl survey CPUE due to variability in oceanic and tidal currents.

Escapement under the footrope of a trawl can have an important effect on capture efficiency (Dickson 1993). Most of this escapement occurs in the center of the trawl, where fish are concentrated as a result of herding (Engås and Godø 1989, Walsh 1992, Ona 1999). Because variation in footrope contact with the bottom in this location is likely to influence escapement, it is important to understand how footrope contact varies with potentially controllable, external factors, such as STW. We examined how STW influenced trawl performance and efficiency with a two-phase experiment. During Phase I, we investigated the relationship between footrope contact and STW for the poly Nor'eastern trawl used by the Alaska Fisheries Science Center (AFSC; Somerton and Weinberg in press). A newly developed bottom contact sensor (BCS) capable of measuring the distance between the footrope and the bottom was used to examine this relationship. During Phase II, we investigated the effect of STW on the capture efficiency of the trawl. This relationship was explored by attaching an auxiliary net under the trawl to capture fish which would have otherwise escaped.

Material and Methods

PHASE I

Trawl operations were conducted with the poly Nor'eastern bottom trawl fit with roller gear customarily used in AFSC assessment surveys of shelf groundfish resources of the Pacific West Coast (California, Oregon, Washington), Gulf of Alaska, and Aleutian Islands (Shaw et al. 2000, Martin 1997, Harrison 1993). This 4-seam, hard bottom trawl is constructed of 127 mm polyethylene stretch-meshed webbing with a 32 mm nylon codend liner. The headrope and footrope are 27.2 m and 24.9 m long, respectively. The roller gear consists of 36 cm rubber bobbins separated by 10 cm rubber disks and is preceded by 5.9 m long wing extensions on each side made up of 10 cm rubber disks. A pair of 1.8 x 2.7 m steel V-doors weighing approximately 800 kg each are connected to the trawl by triple 54.8 m long steel bridles on each side.

Trawling was conducted in September 1999, by the 41 m long, 1750 horsepower, chartered commercial stern trawler, F/V Sea Storm, off the coast of Washington (approximately 47° 09' N, 124° 37' W) at two depth sites, 77 and 146 m, respectively. The bottom at both sites was gently sloped and consisted predominantly of sand and mud. Tows followed depth contours, which were approximately parallel to the prevailing bottom current.

Each experimental replicate consisted of towing the net for 10 minutes at each of 7 target speeds (2.0, 2.5, 3.0, 3.5, 4.0, 4.5, and 5.0 knots SOG) as determined by differential GPS. All tows were made with the codend open. The amount of trawl warp used (275 and 412 m for the shallow and deep sites, respectively) was consistent with scope ratios employed during standard survey work. Wingspread (wingtip to wingtip) measurements were obtained at 3-5 second intervals with a Scanmar acoustic net mensuration system.

Measurements of trawl speed through water were obtained from two independent current meters each mounted to the center of the headrope. The first, was a self contained Nobska modular acoustic velocity (MAV) oceanographic current meter, collected STW data and flow direction at 1 second intervals with a rated accuracy to 0.006 knots. The second, was an acoustically-linked Scanmar grid sensor (GS) that transmitted data to the vessel at 24 second intervals with a rated accuracy to 0.1 knots. The MAV current meter was mounted to the outside of the trawl while the GS current meter lay immediately beneath the MAV on the inside of the trawl. As back-up to the trawl mounted STW systems, an Aanderra oceanographic current meter, that collected current velocity and direction at 5 minute intervals, was moored 3 meters off the bottom in the vicinity of trawling activity. Speed through water was determined indirectly as the vector summation of vessel speed and current velocity.

Footrope distance from the bottom, measured from the underside of the centermost bobbin, was estimated from a bottom contact sensor (BCS) developed at the AFSC (McEntire in prep). The BCS is a self-recording tilt meter, measuring tilt angle from vertical to within 0.5° , placed inside of a protective watertight, stainless steel housing and mounted on top of a 10 x 52 cm steel sled. The entire assembly weighed approximately 12.5 kg (dry weight). One end of the sled was snapshackled to the footrope center so that it pivoted along the vertical plane of the trawl centerline (Figure 1). The other end rested on the seafloor. Changes in the distance of the footrope off-bottom resulted in changes of the angle of the sled. The calibration of the BCS tilt angle to footrope distance off-bottom was performed on a flat surface, in air. The calibration consisted of measuring angles associated with the distances off-bottom varying from 16.5 cm, the distance of the footrope from the bottom when the bobbins lay on a flat surface, to 41.5 cm.

An underwater video camera was used to confirm bottom contact. The system was suspended above the footrope so that at least one of the two centermost bobbins and the trailing edge of the BCS were in view (Weinberg and Munro 1999). Visual estimates of the degree of footrope contact at each target speed on each tow was based on a 5-point scale (5= center bobbins hard on bottom as evidenced by bobbin rotation; 4= center bobbins lightly touching as evidenced by no bobbin rotation but a trailing mudcloud was observed; 3= center bobbins not touching but close as evidenced by no mudcloud trailing the bobbins but a mudcloud observed trailing behind the BCS; 2= no mudcloud trailing the BCS but bottom still in view; 1=bottom no longer visible). The degree of bottom contact for each target speed for each tow was estimated by assigning the above codes to 10 randomly selected 10 second periods and averaging over the 10 scores.

Measured values of MAV, GS, and differential GPS speeds, wingspread and BCS tilt angle were averaged over the time interval of each target speed. To determine if either of the measured STW (MAV and GS) differed from the speed computed from vessel speed and current velocity obtained by the moored current meter, each of the measured STW was regressed on computed speed. The fit of the regression line was compared to the fit of the equality line (zero intercept, unit slope) using an F-test.

A functional relationship between the measured distance of the footrope off-bottom and the tilt angle measured by the BCS was estimated by fitting a quadratic function with multiple regression to the data from the calibration experiment. To test for curvature in the relationship, significance of the squared term was tested with an F-test. To simplify later interpretation of the predicted distance off-bottom, we subtracted the distance of the footrope off-bottom (16.5 cm) when at rest on a flat surface. Thus the distance off-bottom will refer to the distance from the underside of the central bobbins to the seafloor (see Figure 1). Mean value of distance off-bottom within each time interval was determined by applying the estimated function to the mean value of tilt angle. A functional relationship between off-bottom distance and speed through water was estimated by using multiple regression to fit the model: $\text{distance} = a + b(\text{STW}) + c(\text{STW}^2) + \text{depth}$, then testing for significance of the depth term.

PHASE II

The experiment was conducted with an AFSC poly Nor' eastern trawl fit with an auxiliary net, fashioned after the earlier works of Engås and Godø (1989) and Walsh (1991), that attached underneath the trawl to capture fish and invertebrates passing under the footrope. The auxiliary net is constructed with 102 mm stretched-mesh polyethylene webbing and a 32 mm nylon liner in each of its three codends. The 24.8 m long headrope attached to the fishing line of the trawl. The 28 m long footrope consisting of 1.3 cm chain strung through 12.7 cm rubber disks attached to the trawl at the junction of the roller gear and the wing extensions (Weinberg and Munro 1999). Initial gear trials were conducted using the standard 1.8 x 2.7 m V-doors to observe trawl geometry of the combined main trawl and auxiliary net at various trawl speeds. However, after several tows it became apparent that the drag from the auxiliary footrope affected

trawl performance in two distinct ways. First, the wingspread was considerably lower than expected, particularly at higher speeds. To help increase the wingspread we switched to larger doors measuring 2.1 x 3.0 m and weighing 1200 kg apiece. Second, the footrope distance from the bottom was appreciably greater than observed during Phase I, which we suspect was due to the increased drag of the auxiliary footrope. To help stabilize the trawl footrope we added 28.5 kg of weight throughout the 6.1 m center section.

Trawling operations were conducted in late July 2000 aboard the 40 m long, 1525 horsepower, commercial stern trawler, F/V Arcturus. The experimental site was located south of the Pribiloff Islands (55° 36' N, 168° 00' W) in the Bering Sea at a depth of 135 m on a flat, mud and sand bottom. The current generally flows northwestward following the edge but strong cross-shelf tidal activity is also prevalent (Stabenho et al. 1999). Tow direction was parallel to the depth contours unless modified to accommodate sea surface conditions.

Half-hour tows were made using standard survey scope ratios and conducted in sets comprised of one tow at each of the three target speeds, 2.5, 3.0, and 3.5 knots SOG, made in opposing directions, in random order. Each tow began when the target SOG, as determined by standard GPS updated at 2 second intervals, reached equilibrium. The duration to reach such equilibrium ranged from a few seconds to a few minutes after the trawl reached bottom. At the end of each tow, trawl winches were engaged and both engine RPM and variable pitch propeller settings were increased, causing rapid lift of the trawl footrope with the auxiliary footrope following shortly thereafter.

Phase II utilized many of the same synchronized instruments and procedures set forth in Phase I. During all tows wingspread measurements were obtained with a Scanmar net mensuration system and speed through water was measured by the MAV current meter mounted to the center of the headrope on the outside of the net. Footrope distance was measured using the same sled-mounted BCS unit calibrated in 1999, except that an additional 1.9 kg of weight was added to the base of this BCS, to help maintain contact with the bottom at higher speeds. For this experiment we assumed the same distance off-bottom as a function of tilt as measured for Phase I. A second BCS was affixed to the center of the auxiliary footrope and monitored footrope performance of the auxiliary net. A video camera was used during gear trials to ascertain and compare visual bottom contact with BCS tilt angles for both footropes while varying STW. Continuous bottom contact of the auxiliary footrope throughout the experimental speed range was of great concern since estimates of capture efficiency could be compromised if the auxiliary footrope lost bottom contact. To ensure contact, 141 kg of additional weight was placed over the length of the auxiliary footrope and extra BCS units monitored contact at various positions. Bottom contact at the center of the auxiliary footrope, as visually evidenced by mud clouds trailing the groundgear, corresponded to BCS tilt angles of at least 75°. The camera and extra BCS units were removed during tows used for analyses.

The catch from the main trawl and the auxiliary net were processed separately. Flatfish and gadids were sorted by species. Two species of skates, the Alaska skate *Bathyraja parmifera* and the Bering skate *Bathyraja interrupta*, were grouped together as *Bathyraja* spp. Invertebrates and the remaining roundfish were grouped together, respectively. Taxa were weighed and the length of flatfish, gadids, and skates was measured to the nearest centimeter. Biota from completed tows were saved on deck so as not to contaminate catches of subsequent tows.

Measured values of MAV and GPS speeds, wingspread and BCS tilt angle from the two footropes were averaged over the time each footrope spent on bottom as determined from the BCS units. To determine if the auxiliary net altered trawl performance we compared the relationship of wingspread and STW between Phase I, which did not use the auxiliary net and Phase II which did. Wingspread from each

experiment was regressed on STW. Between year differences and differences in the slope coefficients were tested with an F-test using multiple regression. Examination for differences between the footrope distance off-bottom of the two gear types was accomplished by estimating a functional relationship for the Phase II data between the measured footrope distance off-bottom and STW with a quadratic function using multiple regression. Scatterplots of the residuals from the Phase II model and the predicted distance off-bottom based on Phase I model parameters with Phase II data were then explored for trends.

Footrope capture efficiency as a function of STW was examined for three species of flatfish, Arrowtooth flounder *Atheresthes stomias*, flathead sole *Hippoglossoides elassodon*, and Pacific halibut *Hippoglossus stenolepis*, the combined group of skates, and two gadid species, Pacific cod *Gadus macrocephalus* and walleye pollock *Theragra chalcogramma*. For each tow, capture efficiency (E_c), was expressed as:

$$E_c = \frac{CPUE_{\text{trawl}}}{CPUE_{\text{trawl}} + CPUE_{\text{auxiliary}}}$$

with $CPUE_{\text{trawl}}$ and $CPUE_{\text{auxiliary}}$ being numbers of fish caught per square kilometer of area swept. Area swept was computed for each net as the average wingspread times the distance each net fished as determined by BCS.

Since capture efficiency at the footrope can be a function of size (Engås and Godø 1989, Walsh 1992, Munro et al. 1997), capture efficiencies were computed by size categories selected to capture modes or tails in the observed length frequency distributions. Capture efficiency for each species in each size category, was regressed against STW to serve as an aid in discerning trends.

Results

PHASE I

A total of 19 tows were successfully completed (12 shallow and 7 deep). On four tows made with the current the 2.0 knot target speed was abandoned due to poor door performance. This indicates that the slowest speeds used in our study are near the operational limit of the trawl. Camera observations of bottom contact were made during 16 tows, although some of these were unuseable at some speeds due to poor positioning.

Speed through water measured by the MAV current meter was significantly different ($P < 0.001$) than STW computed from vector summation of vessel and current velocities, but the difference was small (Figure 2). Predicted values of MAVS were 0.14 knots less than computed STW at 2 knots and 0.04 knots greater at 5 knots. STW measured by the GS was also significantly different ($P < 0.001$) than the vector computed speed, but in contrast to MAV speed, the difference was considerable. Predicted values of GS speed were 0.44 knots less than the vector computed speed at 2 knots and 0.66 knots less at 5 knots. We interpreted this as indicating that the MAV speed was a good approximation of STW. The MAV current meter broke, however, before the end of the experiment, therefore MAV speed had to be predicted from one of the other STW estimates. Because the residual variance of the regression of MAV speed on GS speed (0.0069) was lower than it was for the regression of MAV speed on vector computed speed (0.0116), MAV STW were predicted for the final 5 tows from GS STW using the regression parameters.

Tilt angles from the BCS ranged from about 63° at the slowest speed to about 30° at the highest speed. However, the tilt angle is a valid indicator of the distance off-bottom only when the trailing edge is

making contact with the bottom. Such contact was determined from observations made with the video camera as evidenced by trailing mud clouds. Based on the speed segments observed, the BCS always maintained contact at angles greater than 38°. In 10 of the 12 cases with tilt angle angles less than 38° the net had lifted to such an extent that the bottom was no longer visible. In all 12 of these cases the distance off-bottom is underestimated by tilt angle.

The predicted value of distances off-bottom as a function of tilt angle from the calibration exercise was quite precise (distance = $47.8152 - 1.0246 \text{ angle} + 0.0041 \text{ angle}^2$; N=39, $R^2=0.999$) under the relatively static conditions under which the measurements were made. Since the squared term of the regression was significant ($P<0.001$), the relationship is slightly curved (Figure 3).

Distance off-bottom increased at an accelerating rate with speed through water. A quadratic model fitted to the data was found not to differ significantly between depths ($P=0.06$), therefore a depth invariant model was chosen (distance = $5.60 - 5.90 \text{ speed} + 1.55 \text{ speed}^2$; N=127, $R^2=0.85$). At STW less than 2.5 knots the center bobbins were in contact with the seafloor, and based on video, were actively rolling (Figure 4). At 3.0 knots, the bobbins were off-bottom by an average of 1.8 cm but were sufficiently close to the bottom to cause a mudcloud. At 3.5 knots the bobbins were off by an average of 3.4 cm. At 4.0 knots the bobbins were off by an average of 6.7 cm and rarely left a mudcloud. At 5.0 knots the bobbins were off by an average of 14.8 cm. However, at speeds near 5.0 knots the BCS itself was often no longer making contact and in most of these cases the bottom was no longer visible.

The pattern of changing wingspread as a function of speed through water was similar at the two depth sites, although the spread was always greater at the deep site (Figure 5). Wingspread initially increased with STW until a maximum was reached at about 2.5 - 3.0 knots, then decreased until a relative minimum was reached at about 4.5 - 5.0 knots. At still higher STW wingspread increased again. Those cases where the footrope had lifted beyond visual distance of the bottom were all associated with the final increase in wingspread.

Phase II

A total of 25 tows were successfully completed. Average STW ranged from about 2.5 to 4.2 knots. Mean tilt angles from the BCS mounted on the trawl footrope ranged from about 43° to 66°; mean tilt angles from the BCS mounted on the auxiliary footrope ranged from about 77° to 86°, all higher than the 75° tilt reading observed during gear trials with a videocamera indicating consistent footrope contact.

As in Phase I, wingspread decreased as a function of increasing STW, although less dramatically with the larger doors and the auxiliary net attached. Variation in wingspread at a given speed rarely exceeded 1 meter over the 2.5 - 4.2 STW speed range fished, similar to the variation during Phase I. Wingspread of the survey trawl as a function of STW with the auxiliary net attached was significantly different ($P<0.001$) than wingspread from the survey trawl by itself, because the straight line fit to the data had significantly different slopes ($P=0.002$; Figure 6).

The predicted values of footrope distance off-bottom as a function of tilt angle obtained in Phase I were used for Phase II. Tilt angles from four tows using these values resulted in negative footrope heights. Footrope heights ranged from -3.1 to 11.7 cm off-bottom. Predicted footrope distance off-bottom as a function of STW was, distance = $33.0 - 24.96 \text{ speed} + 4.70 \text{ speed}^2$ (Figure 7). At 3.0 and 3.5 knots the bobbins were off-bottom by an average of 0.4 and 3.2 cm, respectively, slightly less than observed in Phase I. At 4.0 knots the bobbins were off by an average of 8.4 cm, slightly more than observed in 1999. Residuals determined from the 2000 model less the 1999 expected distances off-bottom are shown in Figure 8. At 3.0 knots, the standard survey towing speed, the two gear types fished similarly, while at 3.2 to 3.7 knots, footrope distance off-bottom was less. At 4.0 knots, instability in the main footrope

increased and off-bottom distance was greater than Phase I.

Capture efficiency as a function of speed through the water varied by species and length group (Table 1; Figure 9). Trawl STW had no effect on Pacific halibut 50-118 cm in length, because 100 percent of the encounters were captured. Speed also did not appear to change the catchability of the two gadid species (Figure 9), because efficiency was 100 percent for Pacific cod and walleye pollock in 20 of the 25 tows in which they were caught. In contrast, catchability was low for skates of all sizes and capture efficiency appeared to decrease with increasing trawl STW. The two larger size categories for arrowtooth flounder (25-55 cm, >55 cm) and the small size category of flathead sole (<25 cm) appear to have been affected by trawl speed (Figure 9).

Discussion

The Alaska Fisheries Science Center conducts a series of bottom trawl surveys that utilize a poly Nor'eastern trawl to sample commercially important groundfish species inhabiting areas with rocky substrate. This trawl was designed to minimize gear damage by reducing the downward pressure in the footrope center, thus allowing the gear to skip over obstructions more easily. Phase I demonstrated, as a consequence of this design, that there is a strong relationship between footrope instability (measured by bottom contact and distance off-bottom) and speed through water. At our standard survey speed of 3.0 knots STW, the central bobbins frequently lost contact, but generally remained close to the seafloor leaving a trailing mudcloud. Footrope contact improved at speeds less than 3.0 knots. However, at STW greater than 3.0 knots contact deteriorated and footrope distance from the bottom increased as STW increased. Between 3.5 and 4.0 knots STW, which is similar to towing into moderate currents, the estimated footrope distances coupled with the existing 13.0 cm clearance for the disks strung between the bobbins created a sizeable gap through which fish could freely pass. At speeds in excess of 4.5 knots STW, or trawling against strong bottom currents, we suspect that the entire net lifts off the bottom and that the distance from the center of the footrope to the bottom may exceed one meter.

Phase II looked at the consequences of degradation in footrope contact on catchability as a function of speed through the water. Towing speeds combined with the affect of local currents provided STW data ranging from 2.5 to 4.2 knots. Preliminary analyses indicate escapement beneath the footrope on catchability was both species and size-specific within this speed range. For the semi-pelagic species, Pacific cod and walleye pollock, that do not necessarily maintain close association with the bottom and enter the trawl sufficiently high to have little escapement beneath the trawl, capture efficiency was not affected by the change in STW. By similar reasoning we hypothesize that escapement beneath the footrope would also remain unaffected by variation in STW for other schooling semi-pelagics species (e.g., *Sebastes* spp.). Catchability also appeared unaffected by trawl STW for large Pacific halibut.

In contrast, for benthic-oriented flatfish and skates, STW did show varying degrees of effect on catchability among three size categories. Munro et al. (1997), Walsh (1992), and others have alluded to a size-dependent relationship associated with the behavioral response to a trawl. Catchability improves with increasing body size since larger fish are able to swim above the level of the footrope more easily but have more difficulty fitting beneath the footrope. It was not surprising, to see the lowest capture efficiencies for smaller arrowtooth flounder, flathead sole, and skates, and that they were most affected by changes in footrope heights. Likewise, it was not surprising to see high capture efficiency for the stronger swimming, moderate sized arrowtooth flounder (25-55 cm), and flathead sole (25-35 cm), and some evidence of decreasing catchability at higher STW, although to a lesser extent for flathead sole.

The reduction in catchability of the large-sized arrowtooth flounder (>55 cm) and skate (> 90 cm) as a

function of increased STW is more difficult to explain. The strongest swimmers can actively search for escape routes and take advantage of these opportunities. However, we also argue, based on video observations, that swimming endurance and fish density in front of the footrope may influence catchability. At slower trawling speeds residence time in the mouth of the trawl increases, as swimmers keep pace with the trawl (Winger et al. 1999). While these fish maintain position, new fish are herded into the path of the trawl, thereby increasing the density of fish in front of the footrope. Increased density fuels confusion and intensifies competition for available hiding and resting areas on the bottom often causing fish to collide (Godø et al. 1999). When larger individuals settle back to the bottom, they displace smaller fish, particularly if they are predators like arrowtooth flounder that actively feed in the path of the trawl. If the footrope distance is sufficiently high off-bottom, such as caused by increasing STW, the large fish have a higher probability of passing underneath and escaping. The displaced individuals, however, return to the water column thus increasing their likelihood of capture. Colliding fish of near equal size frequently end up in the water column, vulnerable to the trawl.

One of the underlying assumptions for using an auxiliary net in catchability studies is that the addition of the capture bag does not perturb the performance of the trawl gear being studied. At this time our analyses on the affect of the auxiliary net are incomplete. Regressions of the wingspreads of the two gear types were significantly different, however in a practical sense this difference is likely unimportant, since peak spread variations differed by only 6% of the total wingspread. Of greater concern was the higher variability in footrope contact of the trawl when the auxiliary net was affixed. The negative values obtained during Phase II suggest that the bobbins penetrated the seabed during some tows. Negative footrope distances could also be explained by improper calibration of the BCS since the individual trawl/footrope combinations differed between the two experiments. Another calibration experiment for the Phase II trawl is planned for this fall.

Our concern for the influence of trawl STW on capture efficiency emanates from the diverse and geographically complex areas we survey where trawling operations are often exposed to strong currents and tidal conditions. Available information on bottom current velocities in the Gulf of Alaska and Aleutian Island areas is scarce, however on the open shelf in the Bering Sea tidal currents can exceed 1.5 knots (Person et al. 1981). Current velocities near and through island passes, prominent land formations, and in conjunction with high relief bottom typically found throughout the Gulf of Alaska and Aleutian Islands can be considerably greater. During normal survey operations decisions on tow direction are based on criteria such as bottom contour, sea state, or location of the next station. Little consideration is given to currents, especially unknown bottom currents. Therefore currents will generate trawl speeds that are both greater and less than our 3.0 knot target speed. Maintaining constant STW, rather than constant SOG, could reduce variability in trawl survey CPUE for some species and sizes due to the affect of water speed on footrope bottom tending performance.

References

- Dickson, W. 1993. Estimation of the capture efficiency of trawl gear. II: Testing a theoretical model. *Fish. Res.* 16:255-272.
- Engås, A. and Godø, O.R. 1989. Escape of fish under the fishing line of a Norwegian sampling trawl and its influence on survey results. *J. Cons. Int. Explor. Mer.* 45:269-276.
- Fridman, A.L. 1986. Calculations for fishing gear designs. Fishing News Books Ltd. Farnham,

- England. 241 p.
- Godø, O.R., Walsh, S.J. and Engås A. 1999. Investigating density dependent catchability in bottom trawl surveys. ICES J. Mar. Sci. 56: 292-298.
- Harrison, R.C. 1993. 1991 Bottom trawl survey of the Aleutians Island area. U. S. Dep. Commer., NOAA Tech. Memo. NMFS-AFSC-12, 144 p.
- ICES. 1999. Manual for the International bottom trawl surveys revision VI. ICES CM 1999/D:2. 49 p.
- Martin, M.H. 1997. Data report: 1996 Gulf of Alaska bottom trawl survey. U. S. Dep. Commer., NOAA Tech. Memo. NMFS-AFSC-82, 235 p.
- McEntire, S. In prep. An instrument to determine time and duration of sea bed contact of a trawl. National Marine Fisheries Service, Alaska Fisheries Science Center, Seattle, WA.
- Munro, P.T., Weinberg, K.L. and Somerton, D.A. 1997. Estimating size-dependent capture rates at the footrope of two different kinds of survey trawls. ICES CM 1997/W06. 18 p.
- Ona, E. 1999. Determining the entrance position of fish in trawls. ICES CM 1999/J:13. 10 p.
- Person, C.A., Mofjeld, H.O. and Tripp, R.B. 1981. Tides of the eastern Bering Sea shelf *In* The eastern Bering Sea shelf: Oceanography and resources. pp. 111-130. Ed. by D.W. Hood and J.A. Calder. U.S. Dept. of Commerce.
- Shaw, F.R., Wilkins, M.E., Weinberg, K.L., Zimmermann, M., and Lauth, R.R. 2000. The 1998 Pacific West Coast bottom trawl survey of groundfish resources: Estimates of distribution, abundance, and length and age composition. U. S. Dep. Commer., NOAA Tech. Memo. NMFS-AFSC-114, 138 p.
- Somerton, D.A. and Weinberg, K.L. In press. The effect of speed through the water on footrope contact of a survey trawl. Accepted Sept. 2000. Fish. Res.
- Stabeno, P.J., Schumacher, J.D., and Ohtani, K. 1999. The Physical oceanography of the Bering Sea *In* Dynamics of the Bering Sea, pp.1-28. Ed. by T.R. Loughlin, and K. Ohtani. University of Alaska Sea Grant, AK-SG-99-03, Fairbanks.
- Walsh, S.J. 1991. Diel variation in availability and vulnerability of fish to a survey trawl. J. Appl. Ichthyol. 7:147-159.
- Walsh, S.J. 1992. Size-dependent selection at the footgear of a groundfish survey trawl. N. Am. J. Fish. Man. 12:625-633.

- Weinberg, K.L. and Munro, P.T. 1999. The effect of artificial light on escapement beneath a survey trawl. ICES J. Mar. Sci. 56:266-274.
- Winger, P.D., He, P.D. and Walsh, S.J. 1999. Swimming endurance of American Plaice *Hippoglossoides platessoides* and its role in fish capture. ICES J. Mar. Sci. 56:252-265.

Table 1. Length categories, the number of fish caught in the main trawl and auxiliary net (in parentheses), and the number of tows having catch in each category for species or taxa of interest.

Taxa	Length (cm)	No. fish	Tows
Arrowtooth flounder	<25	509 (378)	25
	25-55	2791 (165)	25
	>55	181 (20)	25
Flathead sole	<25	451 (233)	25
	25-35	3813 (531)	25
	>35	120 (10)	22
Pacific halibut	51-118	61 (0)	22
Skates	<35	5 (55)	17
	55-75	7 (46)	18
	90-115	37 (67)	23
Pacific cod	50-70	271 (6)	25
Walleye pollock	<21	198 (10)	19
	50-65	420 (6)	17



Figure 1. The bottom contact sensor (BCS) shown mounted to a sled and snapshackled between the centermost bobbins to the steel cable running through the roller gear used with the poly Nor' eastern bottom trawl (net not attached). In this position the cable is 16.5 cm above the floor and the tilt angle of the BCS is approximately 61.5° relative to vertical.

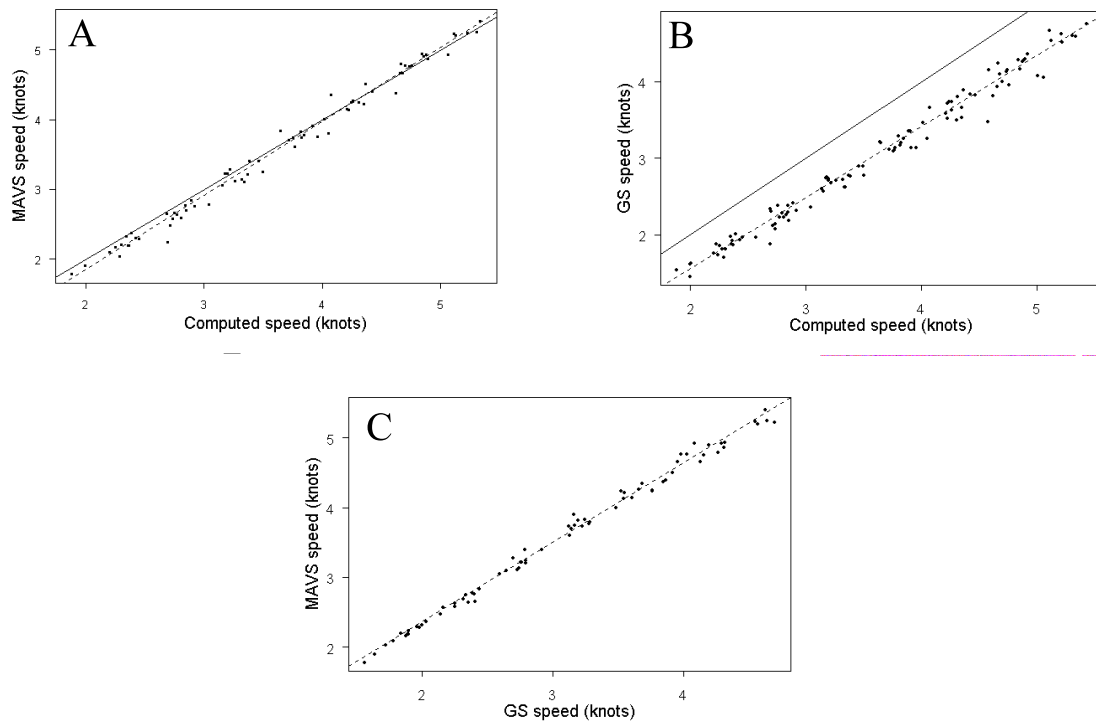


Figure 2. Speed through water (STW) measured by the trawl mounted MAV and GS current meters and STW computed indirectly from vessel velocity and current velocity measured with a bottom moored oceanographic buoy. Solid lines represent the line of equality; dashed line represent the regression of one STW on another. A) MAV STW regressed on computed STW; B) GS STW regressed on computed STW; C) MAV STW regressed on GS STW.

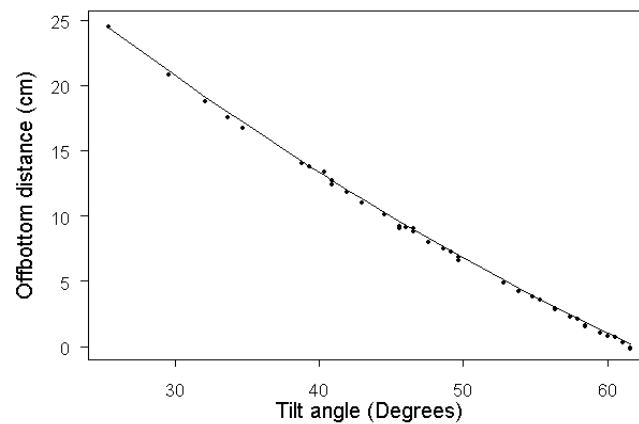


Figure 3. Distance off-bottom plotted against tilt angle measured with the bottom contact sensor for the calibration of the net used in 1999. Calibration was performed on a hard, flat surface.

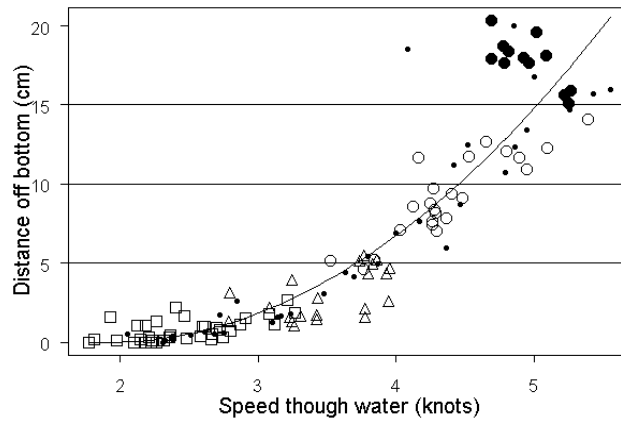


Figure 4. Distance off-bottom, measured beneath the central bobbins, plotted against speed through water. Symbols refer to bottom scores determined by video analysis: square - center bobbin hard on bottom as evidenced by bobbin rotation (score 5); triangle - bobbins lightly touching bottom as evidenced by no bobbin rotation but by the presence of a mudcloud trailing the bobbins (score 4); open circle - bobbins not touching but close to bottom as evidenced by no mudcloud trailing the bobbins, but a mudcloud trailing the BCS (score 3); large filled circle - BCS confirmed off-bottom (scores 1, 2); small filled circle - no visual observation.

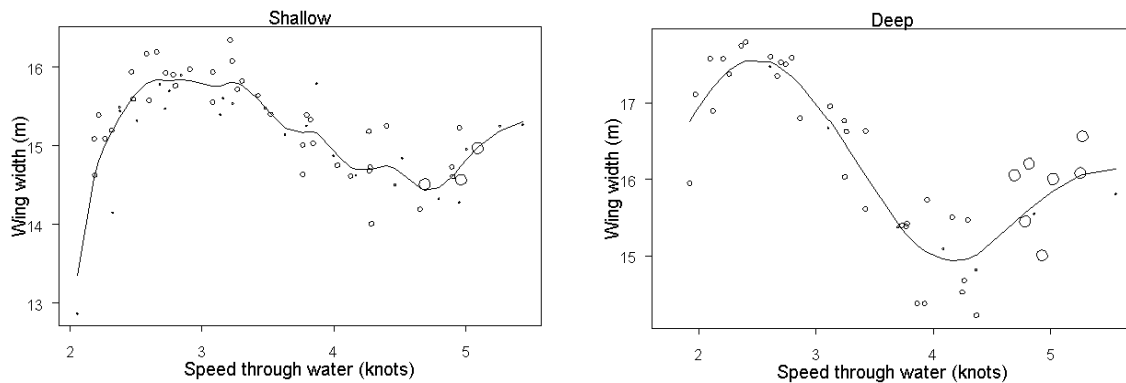


Figure 5. Wing width (wingspread) plotted against speed through the water for the two depth sites. Symbols represent the condition of the bottom contact sensor as determined by video analysis: large circle - BCS confirmed off-bottom; small circle - BCS confirmed touching bottom; dot - no visual observation. The solid line represents a cubic spline fit of the data.

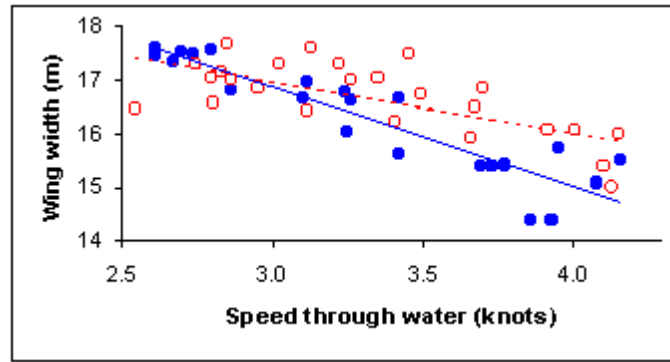


Figure 6. Regressions of wing width (wingspread) plotted as a function of speed through the water (filled circle/solid line - 1999 main trawl only, deep site, open codend; open circle/dotted line - 2000 auxiliary net attached to main trawl, catch contained).

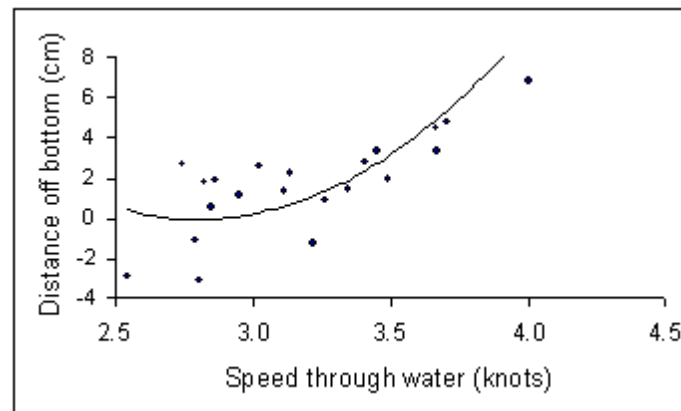


Figure 7. Footrope distance off-bottom of the main trawl when fished with an auxiliary net plotted against speed through the water. The 1999 bottom contact sensor calibration function was fitted to the BCS angles obtained in the 2000 experiment.

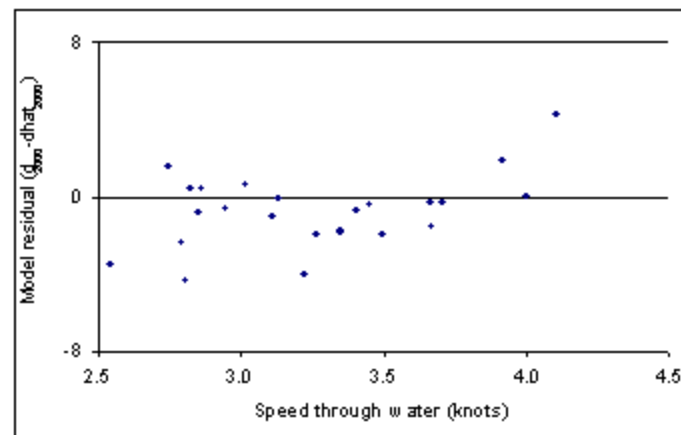


Figure 8. Residuals of the 2000 model (d_{2000}) of estimated distance off-bottom as a function of speed through the water less the predicted distance off-bottom using 1999 model parameters and 2000 experimental data ($d_{\text{hat}_{2000}}$) plotted against speed through the water. The zero line on the Y-axis represents equality.

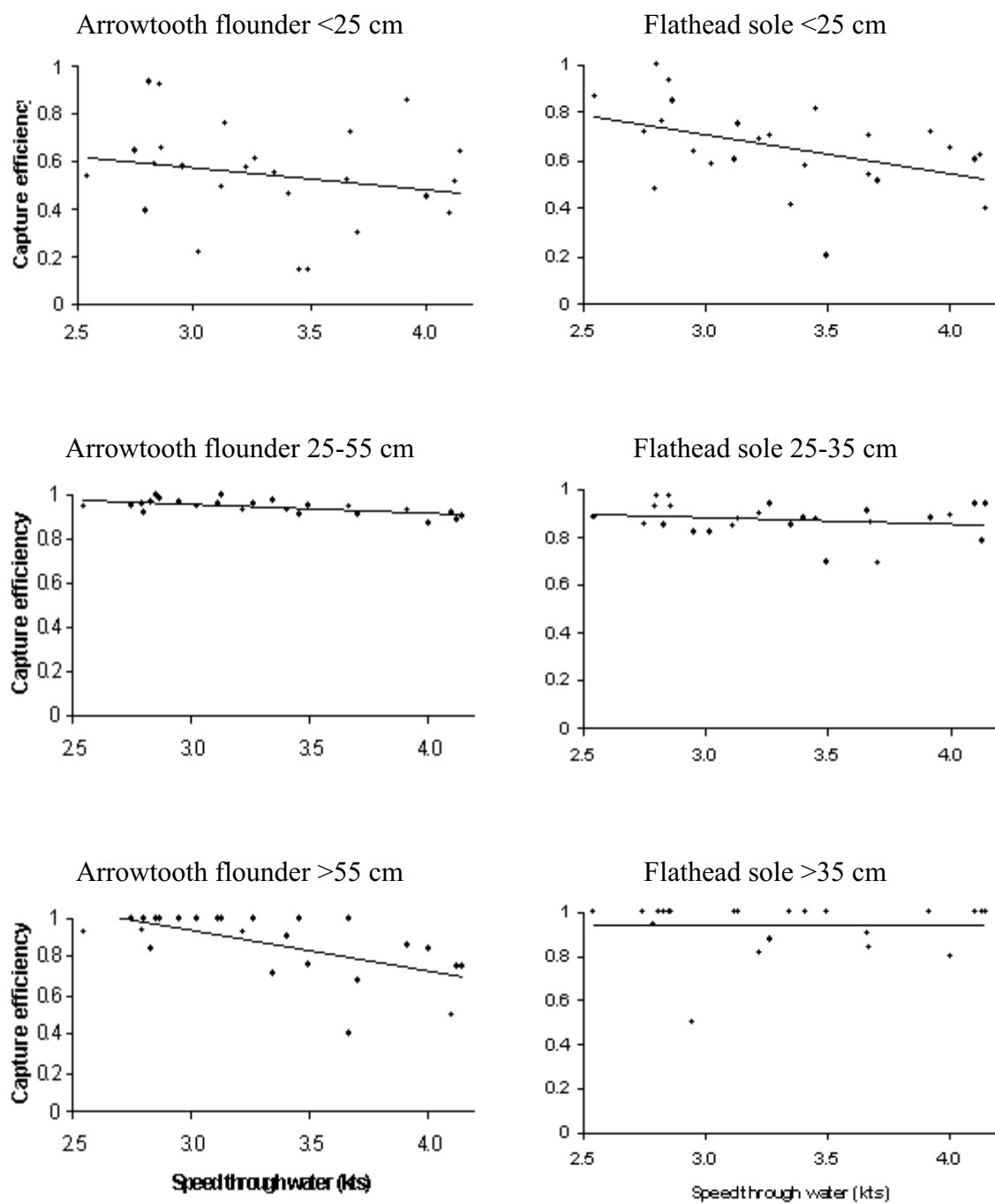


Figure 9. Capture efficiency plotted against speed through the water fit with linear trend line.

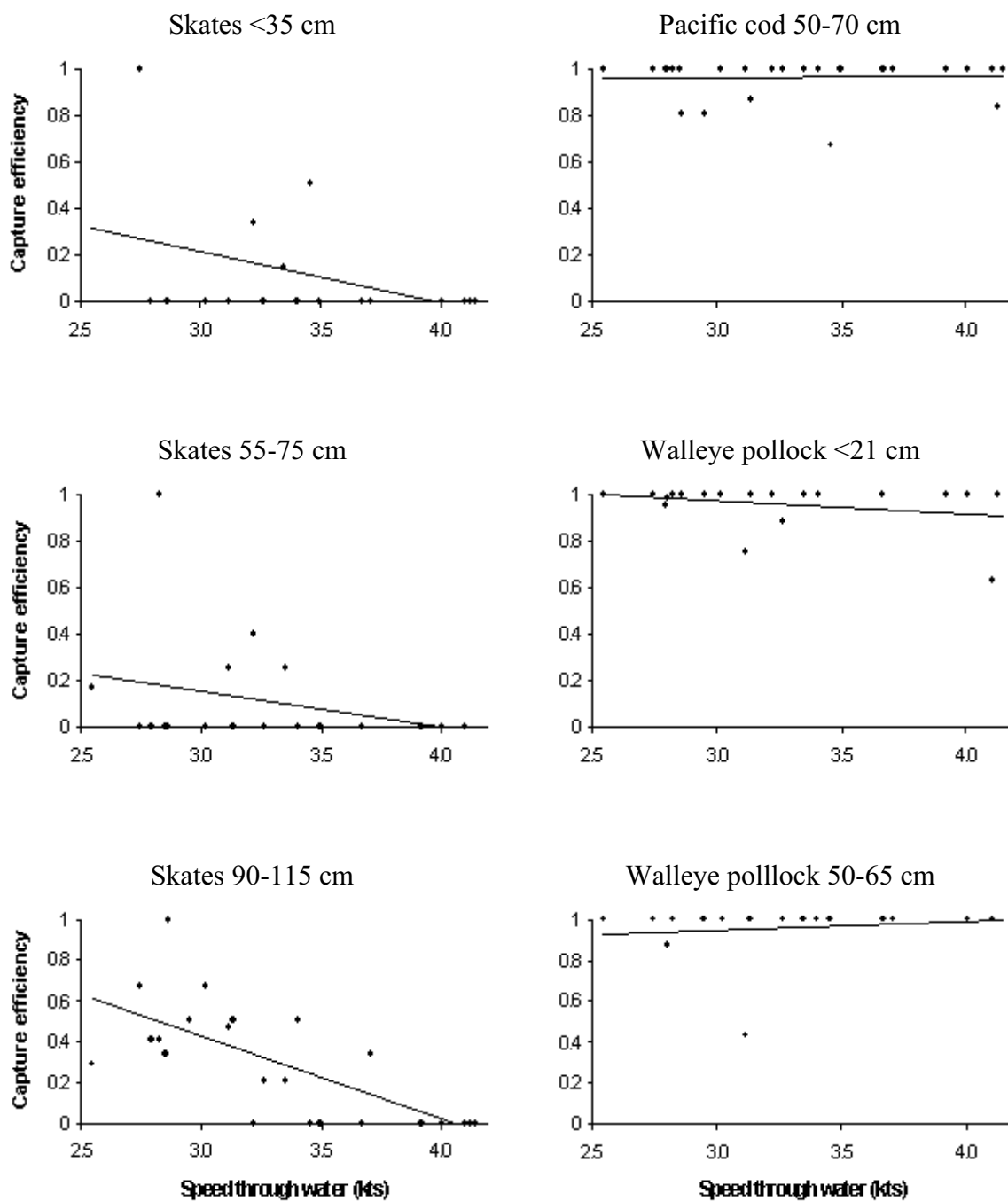


Figure 9. (Cont).